Frustrated smectic layer structures in bent-shaped dimer liquid crystals studied by x-ray microbeam diffraction

Yoichi Takanishi,[1] Megumi Toshimitsu,[1] Michi Nakata,[1] Naoki Takada,[1] Tatsuya Izumi,[1] Ken Ishikawa,[1] Hideo Takezoe,[1] Junji Watanabe,[1] Yumiko Takahashi,[2] and Atsuo Iida[3]

[1]*Department of Organic and Polymeric Materials, Tokyo Institute of Technology, O-okayama, Meguro-ku, Tokyo 152-8552, Japan*

[2]*Department of Physics, Nihon University, Surugadai, Kanda, Chiyoda-ku, Tokyo 101-8308, Japan*

[3]*Photon Factory, Institute of Materials Structure Science, 1-1 Oho, Tsukuba-shi, Ibaraki 305-0801, Japan*

(Received 16 May 2005; revised manuscript received 18 June 2006; published 6 November 2006)

The layer structures in bent-shaped liquid crystal dimers *m*OAM5AMO*m* ($m=6-16$) have been investigated by x-ray microbeam diffraction. These liquid crystal molecules have two rodlike mesogens connected with an odd-numbered alkylene spacer and form a bent shape. In these compounds it is found that the structure changes from the single ($m=6$) to frustrated-layer structures ($m=8$, 10, and 12) and switchable frustrated-layer structures ($m=14$ and 16) with increasing terminal chain length. An anticlinic antiferroelectric structure is suggested in the compound with $m=16$, based on the different electric-field-induced reorientation behavior from those in the other dimers.

DOI: 10.1103/PhysRevE.74.051703 PACS number(s): 61.30.Eb, 61.10.−i

I. INTRODUCTION

Since the discovery of the polar order and its switching in achiral bent-core molecules [1], a variety of studies have been intensively performed. Particularly, the bent shape provides very interesting and attractive aspects to liquid crystal science from the viewpoint of the relationship between system chirality, layer chirality, and molecular chirality [2–7]. Moreover several novel mesophases with different layer structures have been discovered, being designated as B1-B8 [7,8]. The B2 phase, which is a switchable tilted smectic phase, has been studied most extensively. According to clinicity and polarity, structures of the B2 phase are classified into four, namely, $SmC_{(S,A)}P_{(A,F)}$ with the choice of two clinicities, either syn- or anticlinic, and two polarity, either ferro- or antiferroelectric.

The higher temperature smectic phase of pentyloxy and hexyloxy homologous series of prototype molecules is designated as the B1 phase [7,8]. According to x-ray diffraction measurements, two or more reflections are observed at a small-angle region. Hence the B1 phase was first assigned to a two-dimensional frustrated rectangular structure, in which the frustrated plane was speculated to be parallel to the molecular bending plane. On the other hand, a smectic phase with a different two-dimensional structure was reported [9]. In this structure, the frustrated plane is normal to the molecular bending plane, and the phase is designated as $B1_{rev}$. Recently, we clarified that the structure in the B1 phase of P -6-O-PIMB is the same as $B1_{rev}$ [10].

The B3 phase is a less studied phase. The B3 phase was attributed to a highly ordered smectic phase or a crystal phase [8,11] because of many x-ray diffraction peaks in a wide-angle region. Recently, however, a similar dynamic behavior was observed in the B2 and B3 phases by terahertz spectroscopy [12], suggesting B3 to be actually a liquid crystalline phase. The B4 phase exhibits blue-color textures, assignable to twist grain boundary structure [13], and is known to have a strong tendency to form chiral domains spontaneously [14]. The B5 phase was observed in a few compounds, and it has in-plane order in addition to the same symmetry as B2 [7,8]. The B6 phase shows a Sm*A*-like fan-shaped texture, and the layer reflection corresponding to the layer spacing is observed to be less than half of the molecular length. This result strongly suggests an intercalated structure and the molecules are tilted with respect to the layer normal [7,8]. The B7 phase is the most mysterious phase till now. In this phase, various types of domains are observed such as the spiral filament, low birefringent accordionlike stripes, colorful focal conics, banana leaf, and checkerboard textures. Coleman *et al.* proposed an undulated layer structure caused by polarization splay by means of x-ray diffraction, freeze fracture transmission electron microscopy, and depolarized reflection microscopy [15].

In addition to these conventional bent-core molecules, bent-shaped achiral dimers, having two rodlike mesogens connected with a alkylene spacer [see Fig. 1(a)], were synthesized [16], being designated as *m*(O)AM*n*AM(O)*m*. In *m*AM5AM*m* ($m=12$, 14) and 16OAM5AMO16, the antiferroelectric switching was observed as in P-*n*-(O-)PIMB [17]. The smectic structures were investigated in homologous series with various lengths of the terminal chains and a connecting spacer. It was reported that the structure changes from single-layer to frustrated-layer and bilayer structures with the increase of the terminal chain length in compounds with a fixed spacer length [16]. Here the single-layer and bilayer structures refer to the structures with each layer consisting of one mesogenic group (a half molecule) and one molecule, respectively, as shown in Fig. 1(b). The competition between the single layer and the bilayer structures results in the frustrated structure with a two-dimensional density modulation. These structural changes were usually analyzed by macroscopic powder x-ray diffraction measurements [16,18]. However, the crossover between these structures by changing the chain lengths is usually ambiguous because diffraction peaks indicating the frustrated and bilayer structures are quite similar. Microbeam probe is a powerful technique to investigate such structures, which enables us to observe diffraction signals from a single domain [19].

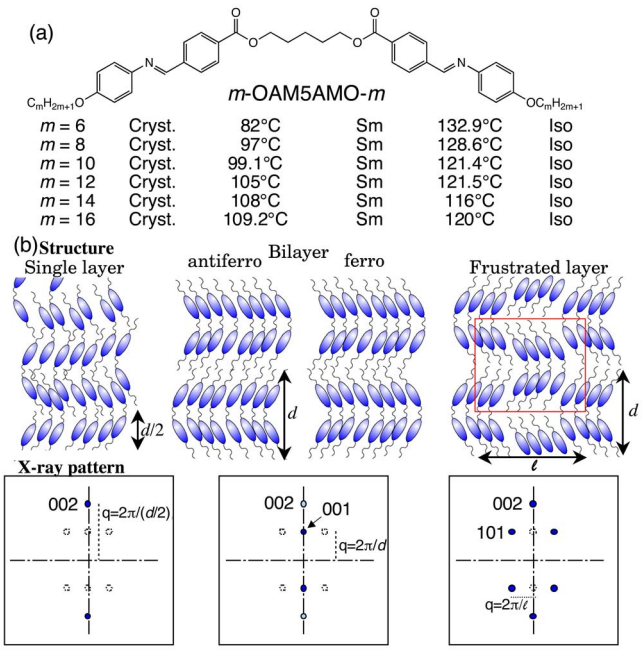

FIG. 1. (Color online) (a) Chemical structure of *m*OAM5AMO*m* (*m*=6, 8, 10, 12, 14, and 16) and their phase sequences. Layer structures realized by bent-shaped dimers are summarized in (b) together with corresponding schematic x-ray diffraction patterns.

We used an x-ray microbeam to perform diffraction measurements on the smectic phase of 8OAM5AMO8, and reported its layer structure and the molecular orientation [20].

In this paper, we focus on three points; (i) For what values of *m*, does the frustrated-layer structure emerge in the compounds *m*OAM5AMO*m*? (ii) Do the molecules tilt with respect to the layer normal? If so, for what values of *m* do they tilt? (iii) Are there any correlations for the appearance of structures between bent-core molecules and bent-shaped dimers? In this paper we present and discuss the results of local layer structures obtained by x-ray microbeam diffraction from uniform domains of homologous series of the bent-shaped dimers, and the crossover among three layer structures (single-, frustrated-, and bi-layer). In addition, the in-plane orientational order is also discussed from the wide-angle diffuse scattering measurements.

II. EXPERIMENTAL

The materials studied are *m*OAM5AMO*m* (*m*=6-16), whose chemical structures and the phase sequences are shown in Fig. 1(a). The sample was sandwiched between two 80-μm-thick glass plates coated with indium-tin oxide. The cell gaps used were 8 and 25 μm for layer diffraction and in-plane diffuse scattering measurements, respectively. No coating and rubbing as made on the substrates for alignment purpose, as this technique is not effective in obtaining the uniform orientation. By gradually cooling the samples from the isotropic liquid, relatively large uniform domains with a diameter of 50~100 μm were obtained except for the dimer

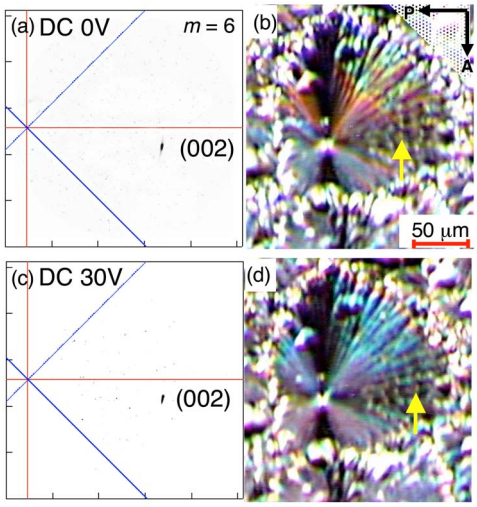

FIG. 2. (Color online) 2D x-ray profiles (a) without and (c) with the application of a DC field (30 V) to a 6OAM5AMO6 sample. Microphotographs (b) and (d) are textures of the cells used for the x-ray experiments. Arrows indicate the irradiated position.

with *m*=14. The temperature stability of the microfurnace was less than 0.3 °C.

The microbeam x-ray diffraction measurements were performed at the Photon Factory on beam line 4A (Tsukuba). The x-ray energy was monochromated to 8 keV (λ =1.55 Å) and 14 keV (λ=0.886 Å) for the layer diffraction and the in-plane diffuse scattering, respectively. The incident beam was monochromated and focused using a double Si/W multilayer monochromator and a Kirkpatrick-Baez focusing system, respectively, with an angular divergence of 0.5 mrad and a spatial resolution of 3×4 μm^2. The detail of the optical geometry is shown in our previous papers [19–21]. In the present measurements, a CCD detector with an image intensifier (Hamamatsu) was used at a diffraction angle corresponding to the layer spacing, $2\theta_B$. The rotation angle of the sample was adjusted to satisfy the Bragg condition, two-dimensional (2D) diffraction patterns were obtained corresponding to the layer structure. Since the intensity of the in-plane diffuse scattering at wide angles was very weak, the profiles were obtained by subtracting the intensity profile of an empty glass cell. Exposure times were 100~300 ms and 360~480 s in the small-angle and wide-angle diffraction measurements, respectively. Camera lengths were about 1800~1900 mm in the layer diffraction measurements and 160 mm in the in-plane diffuse scattering measurements.

III. RESULTS

A. Small-angle diffraction from oriented domains

Figure 2 shows two-dimensional x-ray profiles in the smectic phase of 6OAM5AMO6 before and during the application of an intermediate DC field (30 V). Microphotographs corresponding to each x-ray measurement are shown next to the x-ray data [Figs. 2(b) and 2(d)]. The irradiated position is shown by a yellow arrow in the figures. In the dimer with *m*=6, a single diffraction spot was observed irre-

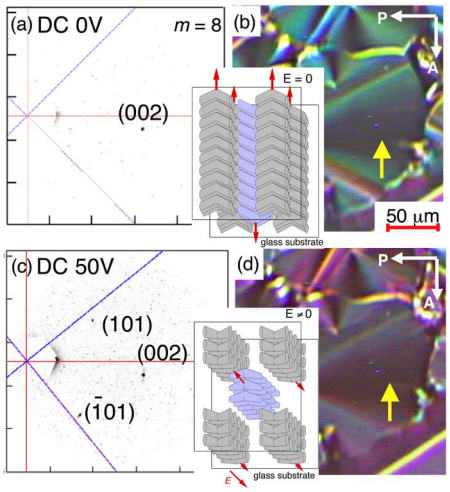

FIG. 3. (Color online) 2D x-ray profiles (a) without and (c) with the application of a DC field (50 V) to an 8OAM5AMO8 sample. Microphotographs (b) and (d) are textures of the samples used for the x-ray experiments. Arrows indicate the irradiated position. Insets of (b) and (d) indicate the molecular orientation with respect to the substrates.

spective of the field application, as shown in Figs. 2(a) and 2(c). The layer spacing calculated from this diffraction is 21.5 Å, which is almost corresponding to half the molecular length calculated by MM2. Hence the peak is assigned to a (002) peak. It suggests that this compound forms a single layer structure, in which molecules randomly intercalate to form a layer consisting of each mesogenic group (half the molecule), as shown in Fig. 1(b) [16].

Quite different x-ray profiles were observed in the dimer with $m=8$, as shown in Fig. 3(c). Before applying an electric field, a single spot (002) corresponding to half the molecular length was observed [Fig. 3(a)] the same as in the compound with $m=6$ [Fig. 2(a)]. Under the application of a DC field, however, additional two spots appear symmetrically with respect to the (002) diffraction spot. These peaks are assumed to be (101) peaks, suggesting that a frustrated layer structure is formed [16]. The diffraction spots, (002) and (101), correspond to 23.1 and 35.4 Å, respectively. In the polarizing microscope observation, color changes were observed, as shown in Figs. 3(b) and 3(d), indicating the increased optical birefringence by the application of a DC field. From these results, we conclude that a molecular reorientation takes place keeping a frustrated layer structure under the application of field, as reported in our previous paper [20]. A possible schematic molecular reorientation is depicted as the insets of Figs. 3(b) and 3(d). Before applying an electric field, the molecular bending plane is parallel to the substrate plane, and the frustrated plane is considered to be normal to these planes, so that the frustrated structure cannot be detected by x-ray diffraction in this geometry. When a field is applied, molecules reorient themselves as the molecular bending plane is normal to the substrate due to the coupling of dielectric anisotropy with the field. Hence (101) peaks indicating the frustrated structure are now able to be detected. The change of color of the texture also supports this model, and in-plane diffuse scattering results are also consistent to this

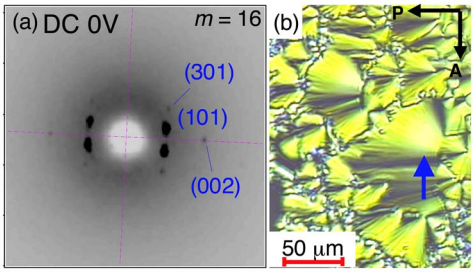

FIG. 4. (Color online) (a) 2D x-ray profiles without applying a DC field to a 16OAM5AMO16. (b) Microphotograph of the texture of the sample used for the x-ray experiments. An arrow indicates the irradiated position. Camera length is circa 400 mm, different from that in Figs. 2 and 3.

model [20], as will be mentioned later [see Fig. 11(c)]. Once the molecular reorientation takes place due to the application of field, the structure remains unchanged even after terminating the field.

Similar results are also obtained in the compounds with $m=10$ and 12. Since the same color change is also observed due to the increase in the optical birefringence, hence similar molecular reorientation takes place as that of the compound with $m=8$, 5 suggesting the frustration remains as such during the application of the field. The distance between (101) and (−101) peak spots decreases with increasing m from 8 to 10 and 12. (002) and (101) diffraction peaks correspond to 24.2 and 43.9 Å for $m=10$, and 25.7 and 48.6 Å for $m=12$, respectively; namely the frustrated lattice is elongated as the terminal chain increases.

In the compound with $m=16$, observed x-ray characteristics were different from those of other dimers. The x-ray profile obtained in the dimer with $m=16$ is shown in Fig. 4. In this dimer, (101) peaks in addition to (002) peaks were observed before applying a field. In addition, (301) peaks were also observed though their intensities were quite weak. Hence the frustrated layer structure was stably formed even in the dimer with $m=16$, although the bilayer structure was suggested to be formed in a previous work [16].

The peak intensity ratios between (101) and (002) obtained from oriented samples of dimers are listed in Table I. It is found that the intensity ratio of the (101) peak to the (002) peak increases with the increase of the terminal chain length. The similar results were observed in the powder x-ray diffraction. This increase indicates that the dimer with $m=16$ has highly modulated layer structure compared with other dimers.

For the compound with $m=14$, we could not obtain uniform domains even for the x-ray microbeam irradiation. In powder x-ray diffraction measurements using the x-ray microbeam, however, a small-angle diffraction peak corre-

TABLE I. Peak intensity ratio between (101) and (002) diffractions of each dimer.

m	8	10	12	14	16
I_{101}/I_{002} (oriented)	0.18	1.31	2.21		5.33

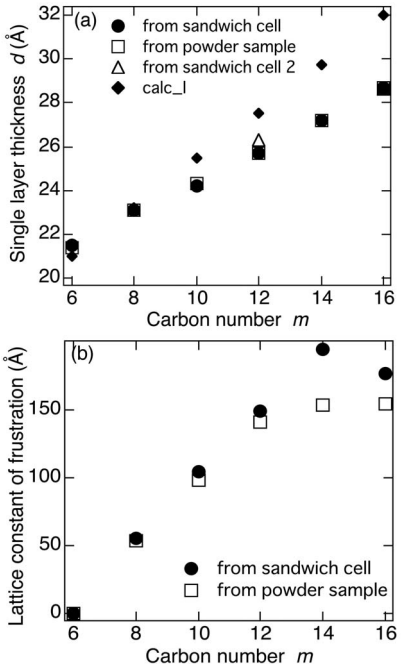

FIG. 5. (a) Single layer thickness and (b) the lattice constant of the frustrated layer structure as a function of the terminal chain length. Closed circles and open squares are results obtained from oriented samples and powder samples, respectively. Powder pattern was also measured from droplet of compounds using an x-ray microbeam. Closed diamonds in (a) are halves of the calculated molecular length. The distribution of values obtained from the same cell structures of the single layer spacing and the lattice constant of the frustration is about ±0.2 and ±1 Å, respectively.

sponding to a spacing of 53.4 Å was observed. Comparing the frustrated structure in the compounds with $m=12$ and 16, it is safely assumed that the compound with $m=14$ also forms the frustrated layer structure.

Figures 5(a) and 5(b), respectively show the single layer spacing, d, and the lattice constant of the frustrated structure, l, as a function of the terminal chain length. The single layer spacing monotonically increases with increasing the terminal chain length, but is deviated from calculated results of half the molecular length (closed diamond) for $m \geqslant 10$. This result suggests that molecules with $m \geqslant 10$ tend to tilt from the layer normal. Although a possible structure of the tilted version of the frustrated layer structure was already shown in Ref. [15], our results were not consistent with the proposed model [15], because neither (001) nor (201) are observed in any compounds. Thus, the tilted frustrated structures in these dimers are different from the modulated ones shown in Ref. [15]. On the other hand, the lattice constant of the frustrated structure, l, monotonically increases for $m \leqslant 12$, and almost saturates at circa 150 Å, suggesting that this length is a critical value to keep the frustrated structure. Details will be discussed later.

B. Intralayer wide-angle diffuse scattering in oriented samples

In order to investigate the intralayer molecular orientation, we measured the wide-angle diffuse scattering. Small-

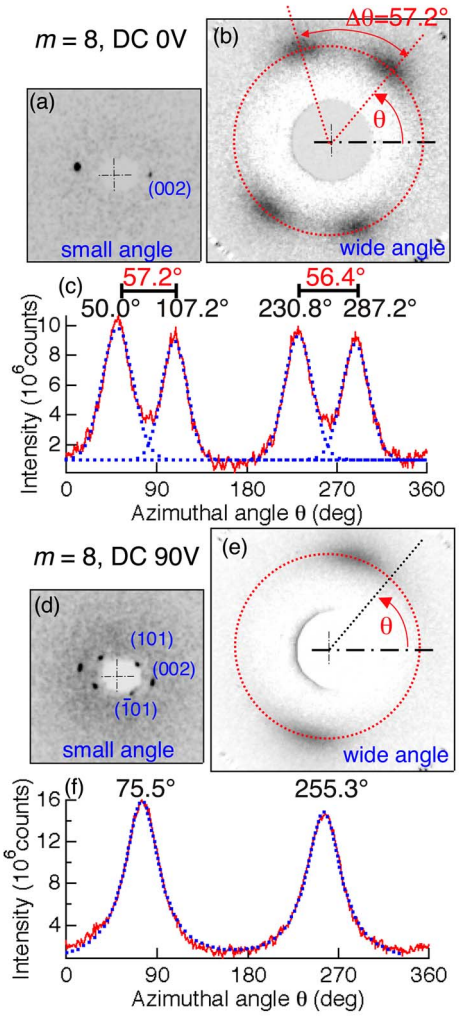

FIG. 6. (Color online) 2D small-angle x-ray profiles of 8OAM5AMO8 (a) before and (d) during a DC field application, and their corresponding 2D wide-angle x-ray diffuse scattering (b) and (e), respectively. The central cross points shown in (a), (b), (d), and (e) indicate the origin. (c) and (f) are intensity profiles as a function of equatorial arc of dotted circles in (b) and (e). Dotted lines in (c) and (f) are fitted curves to the Gaussian functions. Sum of Gaussian functions almost perfectly simulate the experimental results, though not shown.

angle diffraction was also monitored to explore the relationship between the layer direction and molecular orientation, despite of low quantitative accuracy because of a less camera length. Figures 6(b) and 6(e) show two-dimensional wide-angle diffuse scattering patterns obtained from oriented 8OAM5AMO8 before and after the application of a DC field of 60 V/25 μm, respectively. Before applying the field, only (002) peaks appear at small angles, as shown in Fig. 6(a), and four diffuse and broad peaks are observed at wide angles. Figure 6(c) shows the x-ray intensity as a function of the azimuthal angle of the diffuse equatorial arc, θ. Neighboring two broad peaks are symmetric with respect to the layer or the layer normal, and the angle between the nearest peaks, $\Delta\theta$, is circa 57°. When a DC field is applied, (101) peaks appear at small angles, as shown in Fig. 6(d), and the

TABLE II. $\Delta\theta$ determined by the wide-angle diffuse scattering at $E=0$, and $\Delta\theta_{cal}$ determined by MM2 calculation. $\Delta\theta_{cal}$ is the angle between vectors joining C-el to C-ml and C-e2 to C-m2, and $\Delta\theta_{core\text{-}calc}$ is the angle between vectors joining O1 to C-ml and O2 to C-m2, as shown in Fig. 7.

Compounds	$\Delta\theta$	$\Delta\theta_{cal}$	$\Delta\theta_{core\text{-}cal}$
8OAM5AMO8	57.2°, 56.4°	39.6°	65.3°
10OAM5AMO10	59.9°, 59.2°	36.9°	65.3°
12OAM5AMO12	47.4°, 53.1°	33.9°	65.3°
16OAM5AMO16	45.3°, 47.2°	30.4°	65.3°

wide-angle diffuse scattering pattern changes from four peaks [Fig. 6(b)] to two peaks [Fig. 6(e)], which are also symmetric with respect to the layer normal, as clearly displayed as an azimuthal angle dependence in Fig. 6(f). This diffuse peak corresponds to the spacing of circa 4.3 Å, which is almost independent of the applied field. It is noticed that both the wide- and small-angle diffraction patterns are consistent to the nontilted frustrated structure.

For wide-angle scattering measurements, similar results are also observed in the compounds with $m=10$ and 12 as in 8OAM5AMO8. A considerable difference is noticed in the values of $\Delta\theta$ before applying the field, and $\Delta\theta$ gradually decreases with increasing the terminal chain length, as summarized in Table II. When a field is applied, the four diffuse peaks change into two in both the compounds the same as observed in 8OAM5AMO8. The wide-angle diffuse scattering also indicates that the average molecular long axis is directed normal to the layer irrespective of the applied field. The intralayer molecular spacing is almost the same as that of 8OAM5AMO8.

Figure 7 shows the chemical structure of 8OAM5AMO8 determined by a simple MM2 calculation. The methylene group is flexible to some extent and some rotational freedom may exist. However, Abe [22] already showed that the anticlinic structure of the rigid cores connected with an odd-numbered methylene group is stable, and it is actually confirmed in some dimers connected with odd-numbered methylene spacers such as BB-n [23] and homologues of dimeric TFMHPOBC [24]. Hence the bent-shaped structure of our dimers is considered to be fairly stable, too. From our calculation, the angles between two mesogenic long axes (α) are estimated to be circa 115° and 140° depending on the cases that the mesogen is regarded as only a rigid core or as a rigid core with a terminal chain, respectively. In addition to $\Delta\theta$ determined experimentally, $\Delta\theta_{core\text{-}calc}(=180°-\alpha)$ and $\Delta\theta_{calc}$ in each dimer which are the angles defined by Fig. 7

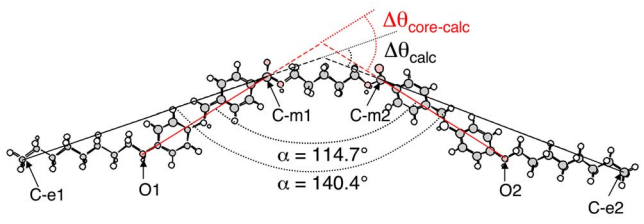

FIG. 7. (Color online) Calculated chemical modeling of 8OAMA5AMO8. $\Delta\theta_{cal}$ and $\Delta\theta_{core\text{-}cal}$ in Table II are defined geometrically.

are also listed in Table II. The fact that $\Delta\theta$ is close to $(\Delta\theta_{calc}+\Delta\theta_{core\text{-}calc})/2$ strongly suggests that the wide-angle diffuse scattering originates from the orientational distribution of each mesogenic part (half the molecule) in a layer. Hence for the compounds with $m=8-12$ before applying an electric field, $\Delta\theta$ comes from the mesogenic bending angle of each molecule and thus the molecular bending plane is parallel to the substrates, as shown in the inset of Fig. 3(b). Hence observed four diffuse peaks indicate the anticlinic orientation of mesogenic parts. On the other hand, the bending plane stands up with respect to the substrates due to the application of field, so that two diffuse peaks [Fig. 6(e)] corresponding to the intralayer spacing between bending planes of neighboring molecules are observed normal to the small-angle diffraction spots.

Let us now consider the compound 16OAM5AMO16. Slightly different characteristics from the other dimers with $m=8$, 10, and 12 were obtained in 16OAM5AMO16, as shown in Fig. 8. First, the (101) diffraction peaks are observable irrespective of the field application, as seen in Fig. 4. If it is assumed that the molecular orientation is such as shown in the inset of Fig. 3(b), then the (101) diffraction spots should not emerge. On the other hand, if it is assumed that the molecular orientation is such as shown in the inset of Fig. 3(d) to explain the emergence of the (101) diffraction, then the wide-angle profile should not split. However, experimentally it is not the case, i.e., the wide-angle diffraction profile splits, as shown in Fig. 8(c), contradicting the structure shown in Fig. 3(d). In order to obtain further information on the structure of the compound 16OAM5AMO16, x-ray diffraction measurements were carried out under a high electric field. By the application of an intermediate field (DC 60 ~ 200 V/25 μm), no obvious change of extinction direction was noted from the texture observation. However, the further increase of field (±300 V/25 μm) results in the rotation of the extinction direction. In the previous electrooptic measurements, an apparent optical tilt angle was reported as 13° [25]. Figure 9 shows the wide-angle diffraction intensity profiles as a function of equatorial arc obtained from a partially oriented sample of 16OAM5AMO16 during the application of a high square-wave voltage (±300 V/25 μm at 5 Hz). In these wide-angle diffuse scattering measurements under a large square-wave voltage, a time-resolved method was adopted for obtaining the scattering intensity at each half cycle of the square wave. Since the layer rotation [26] took place under the application of high electric field for a long time, we must decrease an accumulation time to 200 s. In

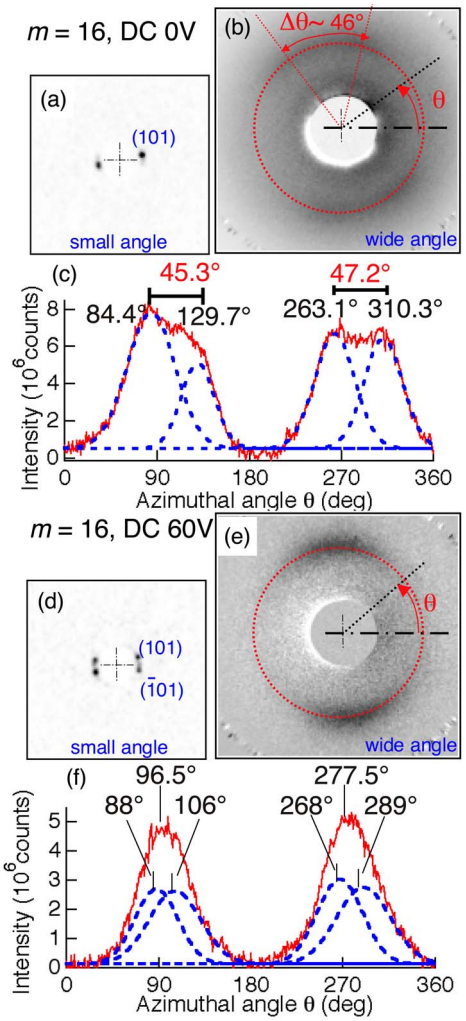

FIG. 8. (Color online) 2D small-angle x-ray profiles of 16OAM5AMO16 (a) before and (d) during a DC field application, and their corresponding 2D wide-angle x-ray diffuse scattering (b) and (e), respectively. The central crosspoints shown in (a), (b), (d), and (e) indicate the origin, (c) and (f) are intensity profiles as a function of equatorial arc of dotted circles in (b) and (e). Dotted lines in (c) and (f) are fitted curves to the Gaussian functions. Sum of Gaussian functions almost perfectly simulate the experimental results, though not shown.

addition, to confirm that the layer rotation did not take place, time-averaged small-angle diffraction measurements were performed before and after obtaining the time-resolved wide-angle diffraction. In this way, we could safely confirm no layer rotation, though a peak/background ratio of the wide-angle diffraction is not as good as that in the other experiments. As noticed from Figs. 9(a) and 9(b), a pair of diffuse peaks is observed and rotates by about 19° by reversing the direction of the applied field. This result clearly indicates that molecules or mesogenic parts tilt synclinically from the layer normal at least under the application of high field. The measured tilt angle is about 9.5°, which is close to the apparent optical tilt angle (13°).

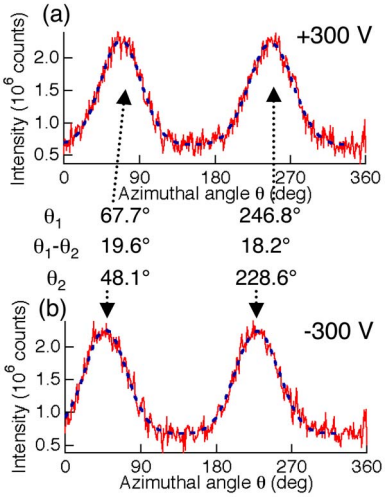

FIG. 9. (Color online) Wide-angle diffraction intensity profiles as a function of equatorial arc at (a) $E=+300$ V/25 μm, and (b) $E=-300$ V/25 μm. The small-angle diffraction spot positions did not change by the field reversal, indicating no layer rotation. θ_1 and θ_2 are azimuthal angles of the wide-angle x-ray peak positions under the positive and negative field application, respectively.

IV. DISCUSSION

A. Orientational order of each mesogen

For uniaxial rodlike molecules, the orientational order parameter based on the Maier-Saupe mean-field theory can be calculated using the wide-angle diffuse scattering data [27]. In the bent-shaped dimers, the wide-angle diffuse scattering data are governed by the order of the mesogenic parts. Therefore, we can evaluate the orientational order of the mesogenic group using the averaged half width at half maximum (HWHM) of the diffuse peaks decomposed from the experimental profiles, assuming Gaussian functions. The results are summarized in Table III. Since the decomposition can be successfully made in the absence of a field in all the dimers [see Figs. 6(c) and 8(c)], the order parameters were properly evaluated, which are also listed in Table III. In 8OAM5AMO8, HWHMs are 18.4° and 20.6°, which correspond to 0.76 and 0.70 in the order parameter under the Maier-Saupe mean-field theory, in the absence and presence of a field, respectively. Thus, the orientational order in the smectic phase of 8OAM5AMO8 is comparable to that in the Sm*A* phase of rodlike molecules. With increasing the terminal chain length, HWHM increases, suggesting the decrease of the orientational order, i.e., 0.76 ($m=8$), 0.72 ($m=10$), 0.65 ($m=12$), and 0.55 ($m=16$). Under an electric field, however, the decomposition of the diffraction peaks is not easy, particularly in tilted dimers of 16OAM5AMO16 [see Fig. 8(f)]. Moreover, four mesogenic groups in adjacent layers have four different orientations in the anticlinic layer structure. Therefore, we did not estimate the order parameter of the mesogenic groups under an electric field and just listed their HWHMs.

We discuss the possible reasons of decreasing tendency of the orientational order with increasing the terminal chain length and by applying an electric field, as summarized in

TABLE III. Average values of HWHM of the wide-angle scattering peaks of each dimer before and during a field application. The order parameter S of the mesogenic group was estimated from the HWHM in the absence of an electric field and is also listed.

Compounds	Field Conditions	Average HWHM	S
8OAM5AMO8	E=0 V	18.4±1.5°	0.76
	E=90 V	20.6±0.8°	
10OAM5AMO10	E=0 V	19.8±1.0°	0.72
	E=90 V	31.1±2.3°	
12OAM5AMO12	E=0 V	22.4±2.2°	0.65
	E=60 V	36.4±3°	
16OAM5AMO16	E=0 V	26.5±2.1°	0.55
	E=60 V	32.3±2°	
	E=100 V	31.1±2.1°	
	E=200 V	35.4±2.3°	
	E=300 V	34.4±2.2°	

Table III. First, why does the order parameter decrease with increasing the terminal chain length? The three physical quantities, which change with increasing the terminal chain length, are (i) decreasing biaxiality of molecules, (ii) increasing disorder of the terminal groups of molecules, and (iii) increasing anticlinic molecular tilt with respect to the smectic layer normal. The decreasing biaxiality (i) may enhance the rotational fluctuation around the molecular long axis (the main axis of the moment of inertia). If it is assumed that the core structure is independent of the terminal chain length, orientational order of the mesogenic part should decrease upon increasing rotational fluctuation. It is natural to consider that the increasing disorder of the terminal groups (ii) bring about the disorder of the mesogenic part. The increasing molecular tilt (iii) cannot be disregarded. As seen in Fig. 5(a), the layer spacing deviates from the calculated molecular length, and the difference becomes larger particularly in the compounds with $m>12$, strongly suggesting that molecules with large m are tilted from the layer normal. This small tilt of molecules and the associated molecular fluctuation around the tilting cone are effective to decrease the orientational order. Thus all the changes of the three physical quantities with increasing terminal chain length lead to a lower orientational order of the mesogenic group, as experimentally observed.

Secondly, for the decrease of the orientational order due to the application of field, two possible reasons may be pointed out; (i) the hydrodynamic flow and (ii) the rotational fluctuation around the molecular long axis. The reason (i) i.e., electrohydrodynamic effect [28] is particularly important when a high field (±300 V/25 μm) is applied to the compound with m=16. However, at least it was confirmed by small-angle x-ray diffraction that the layer reorientation hardly takes place. For dimers with m=8–12, it is not easy to explain that the decreasing order is due to the electrohydrodynamic effect because the applied field is relatively low (60~90 V/25 μm) and the textures are stable under the application of a field. A better explanation is required for the reason (ii). First, it should be noted that the direction of the bending plane changes due to the application of a field. This reorientation of bending plane is important, since the x-ray observation is always made along the field direction (cell surface normal). The bending plane of the bent-shaped dimers is more or less parallel and perpendicular to substrate surfaces in the absence as well as in the presence of an electric field, respectively. Hence the projected components of the mesogenic group onto the substrate plane change tangentially and linearly by the rotational fluctuation of bent-core molecules about the molecular long axis in the absence and presence of an electric field. Therefore, even if the same fluctuation occurs in the absence and presence of an electric field, the order parameter is more seriously influenced by the fluctuation under the electric field. This may give rise to the reduced value of orientational order under the electric field.

B. Phase structures

Based on the present experimental results, phase structures of mOAMnAMOm(m=6-16, n=5) as a function of end-chain length are shown in Fig. 10, which is a revised version of the previous one [16]. Dotted lines are boundaries between single, frustrated, and bilayer structures in our previous paper. Solid ones are revised ones, and the regions of frustrated and switchable frustrated structures are classified

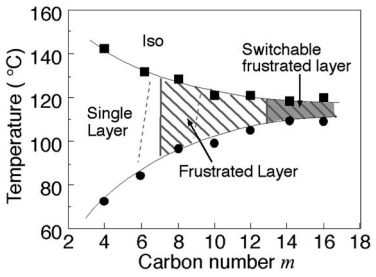

FIG. 10. Phase sequences as a function of terminal chain length. Fine dotted lines indicate the previous result showing the phase boundaries among single-layer, frustrate-layer, and bilayer structures. A hatched area indicates a frustrated-layer structure, and gray colored area indicates a switchable phase.

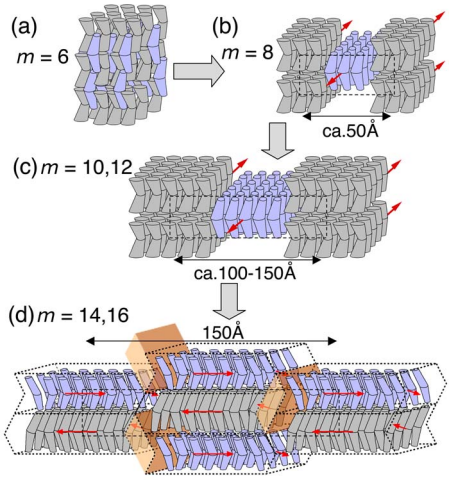

FIG. 11. (Color online) Layer structure change depending on the terminal chain length. m is the carbon number of terminal chains. Dashed lines of (b) and (c) indicate a unit of frustrated structure while that of (d) is a half of the unit structure. Brown colored areas of (d) indicate low density regions.

by hatched and hatched-gray patterns, respectively.

Figure 11 schematically illustrates the layer structures for different terminal chain length. This type of layer formation is considered to be governed by the competition between polarization stability and molecular packing stability. In the compounds with short terminal chains, the intermolecular rigid core interaction is rather strong because the flexible terminal chain hardly disturbs the orientation of the rigid core. Hence one of the mesogenic groups of each dimer can intercalate randomly, and as a result the single-layer structure is formed. This structure is also stable from the viewpoint of no macroscopic polarization because of the equally opposite orientations of polarizations in the bent plane. For mesogenic groups to form this layer structure, $m=n$ seems to be the most appropriate condition. From this viewpoint, for the compound with $m>8$, where m is much larger than $n(=5)$, the mesogenic groups are impossible to intercalate to each other and to form the single-layer structure. Hence, although the molecular packing locally changes to the bilayer structure, the frustrated structure remains more stable because the macroscopic polarization is cancelled out and each mesogen in a layer prefers to orient to the same direction due to the packing entropy. Similar change from the intercalated structure to the frustrated one with increasing the terminal chain length was also confirmed in bent-core molecular systems by several groups [29–31]. In their papers, the B6 phase having the intercalated structure changes to the B1 phase having the 2D structure with the increase of the terminal chain length, though molecules are tilted from the layer normal in both the phases [8,29,32–34].

When the terminal chain length becomes much longer, the aliphatic interaction becomes stronger and the phase separation between alkoxy chains and rigid mesogen cores easily occurs. As a result, the bilayerlike structure may become more stable than the frustrated one, so that the lattice constant of frustration becomes larger. Actually, in the bent-core molecular system mentioned above, the B2 phase appears when the terminal chain becomes longer. In contrast, we could not see a distinct crossover point between frustrated and bilayer structures in the present dimer system, although the molecular tilt angle seems to increase gradually with the chain length. According to Fig. 5(a), molecules begin to tilt when $m=10$. However, an antiferroelectric tristable switching was optically observable only in the compounds with $m=14$ and 16 [18,25]. This is consistent to the present result; i.e., diffraction patterns observed in dimers with $m=8-12$ are different from that in the dimer with $m=16$.

Then what happens in the compound with $m=16$? As shown in Fig. 5(b), the size of the layer block (lattice constant, layer column) gradually increases as the increase of the terminal chain length and saturated to circa 150 Å, which must be a critical value for a stable formation of the frustrated structure. As shown in Fig. 9, synclinic structures are realized under the high positive or negative field. Since (101) peaks suggesting the frustrated structure are observable in the absence of a field, as shown in Fig. 4, the splitting of the wide-angle diffraction peak shown in Fig. 8(c) cannot be assigned to the same origin as in *m*OAM5AMO*m* ($w=8$, 10, and 12), i.e., the individual orientation of two mesogenic groups connected by an alkylene linkage [see Fig. 1(a)]. On the other hand, if we ascribe these split wide-angle diffraction peaks to the alternately tilted molecular orientation, the splitting angle ($\Delta\theta\sim 45°$) is clearly larger than the molecular tilt angle determined by Fig. 9 (9.5°) and/or the apparent optical tilt angle (13°). A possible structure satisfying these conditions before applying an electric field is illustrated in Fig. 11(d), an anticlinic structure is evident from Fig. 8(c), in which average wide-angle diffraction peaks are located along the layer normal and each peak seems to be decomposed into two peaks, as shown by dotted lines. The structure is similar to the polarization-modulated structure reported in [15], except that the clinicity is anticlinic. Brown boxes in Fig. 11(d) may be the region of lower molecular density than the other part, or may be filled with polarization splayed structures, as shown in Ref. [15]. The details are our future problems to be resolved.

Based on the x-ray and electrooptical results, we propose the change in structure of the compound with $m=16$ due to the application of an electric field, as shown in Fig. 12. Under the application of an intermediate field ($E=60-200$ V/25 μm), the bend direction of dimers orients parallel to the field due to the dielectric anisotropy [see Fig. 12(b)]. Since the orientational order parameter of mesogenic groups is low, two peaks of the wide-angle diffuse scattering caused by the anticlinic layer structure with a tilt angle of 10–13° are considered to be superimposed. As shown in Fig. 8(f), the intensity profile can be decomposed into two peaks based on the assumption that mesogen aligns anticlinically with the tilt angle of circa 20° as indicated in Fig. 12(b). In other words, the splitting in diffused peak profiles shown in Figs. 8(b) and 8(c) is caused by the anticlinic structure of mesogenic parts of bending dimers, while that shown in Figs. 8(e) and 8(f) comes from the anticlinic molecular tilt from the layer normal. With further increasing field to 300 V/25 μm, molecules tilted synclinically due to the field-induced phase transition from the antiferroelectric state to the ferroelectric state, are shown in Figs. 12(c) and 12(d).

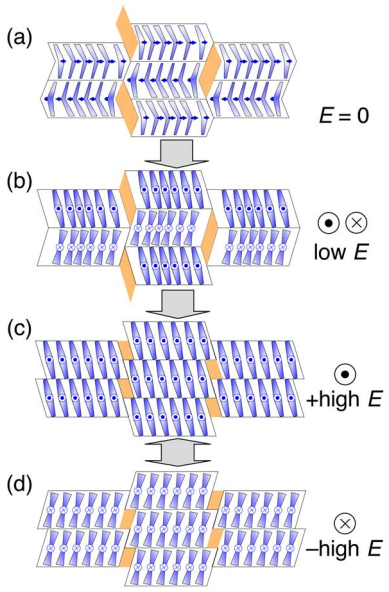

FIG. 12. (Color online) Proposed layer structure change in 16OAM5AMO16 depending on an applied field; initial state ($E=0$) (a), the state under an intermediate field application (b) and the state under the application of (c) positive and (d) negative high field. Brown colored areas of (a) and (b) indicate low density regions.

The structure is similar to that of the synclinic $B1_{revtilt}$ phase [35]. In such a structure, it is natural to consider that (101) and (-101) spots should not be symmetric to the (002) direction, though some exceptional results are reported [34,36]. Unfortunately, we are unable to obtain any further information from the small-angle diffraction because of the low resolution. The details will be our future problem.

Finally we discuss the relation between the single-layer, frustrated and bilayer structures observed in the present work and B1-B7 structures observed previously in bent-core molecules. A single-layer structure corresponds to the B6 phase [8], a frustrated one is quite similar to the $B1_{rev}$ phase [10], and the smectic phase of 16OAM5AMO16 is a kind of $B1_{revtilt}$ phase. Indeed the similar sequential change of the structure (B6-B1-B2) depending on the end chain length is also reported in the bent-core molecular system [29–31]. In Ref. [31], the origin of this change was explained by considering the relation between the free space and terminal chain length based on the eletrostatic potential calculation. However, it is not straightforward to identify the correspondence of the layer structures in the two systems, i.e., bent-core mesogens and bent-shaped dimers. Most important point in the present systems is the existence of an alkylene spacer. Two mesogenic parts are connected by a flexible alkylene group in bent-shaped dimers, whereas a hard core part such as a phenyl ester group links two mesogenic parts in the so-called banana mesogens. In the bent-shaped dimer, moreover, the aliphatic interaction of an alkylene group of the spacer with terminal alkoxy chains is also effective in comparison with the polar interaction. This difference may also be reflected in the molecular tilting. In the bent-core molecular systems, molecules are tilted in a layer in both the B6 and B1 phases [8,29,32–34], whereas the molecules are not tilted in the single-layer and frustrated-layered phases of dimers with $m=6-10$. The structural change of dimers, depending on the terminal chain length, can be explained by the balance between the lengths of the alkylene spacer and the terminal alkoxy chain, as mentioned above. Hence the mechanism of the formation of these structures seems to be different from those in the bent-core mesogens, although the phase and their layer structure emerging in bent-shaped dimer mesogens are similar to B6, $B1_{rev}$, and B7 phases in bent-core mesogens.

V. CONCLUSIONS

We studied the local layer structures of bent-shaped dimers mOAM5AMOm ($m=6-16$) using x-ray microbeam diffraction and discussed the relation among each layer structure, its stability and the terminal chain length. Clear diffraction patterns were obtained from the uniform domains. The compound with $m=6$ was concluded to exhibit the single-layer structure, whereas the compounds with $m=8$, 10, and 12 show the frustrated layer structure. The highly ordered smectic layer blocks (columns) are formed in the compounds with $m=16$, which is quite different from that in the compounds with $m=8-12$ in the viewpoints that it is a tilted phase and is switchable under an electric field. Frustration of the layer structure is discussed based on the phase sequence as a function of the chain length obtained by the present x-ray studies. Molecular orientational order is also discussed from the wide-angle diffuse scattering and the order is very high in the compounds with small m's and gradually decreases with increasing the chain length.

ACKNOWLEDGMENTS

We are very thankful to N. Yamamoto for his technical assistance in making the microfurnace to control the sample temperature. This work is partly supported by Grant-in-Aid for Scientific Research (S) (16105003), (B) (16350070), and on Priority Area (B) (12129202), and for the Encouragement of Young Scientists (16350070), the Ministry of Education, Science, Sports and Culture. This work was carried out under the approval of the Photon Factory Advisory committee (Proposals No. 00G088 and No. 02G135). We are also thankful to Surajit Dhara for his critical reading.

[1] T. Niori, T. Sekine, J. Watanabe, T. Furukawa, and H. Takezoe, J. Mater. Chem. **6**, 1231 (1996).
[2] D. R. Link, G. Natale, R. Shao, J. E. Maclennan, N. A. Clark, E. Körblova, and D. M. Walba, Science **278**, 1924 (1997).
[3] D. Shen, S. Diele, G. Pelzl, I. Wirth, and C. Tschierske, J. Mater. Chem. **9**, 661 (1999).
[4] J. Thisayukuta, Y. Nakayama, and J. Watanabe, Liq. Cryst. **27**, 1129 (2000).
[5] G. Pelzl, S. Diele, S. Grande, A. Jakli, Ch. Lischka, H. Kresse, H. Schmalfuss, I. Wirth, and W. Weissflog, Liq. Cryst. **26**, 401 (1999).
[6] H. Niwano, M. Nakata, J. Thisayukta, D. R. Link, H. Takezoe, and J. Watanabe, J. Phys. Chem. B **108**, 14889 (2004).
[7] H. Takezoe and Y. Takanishi, Jpn. J. Appl. Phys., Part 1 **45**, 597 (2006).
[8] G. Pelzl, S. Diele, and W. Weissflog, Adv. Mater. (Weinheim, Ger.) **11**, 707 (1999).
[9] J. Szydlowska, J. Mieczkowski, J. Matraszek, D. W. Bruce, E. Gorecka, D. Pociecha, and D. Guillon, Phys. Rev. E **67**, 031702 (2003).
[10] Y. Takanishi, H. Takezoe, J. Watanabe, Y. Takahashi, and A. Iida, J. Mater. Chem. **16**, 815 (2006).
[11] J. Thisayukta, H. Takezoe, and J. Watanabe, Jpn. J. Appl. Phys., Part 1 **40**, 3277 (2001).
[12] Y. Takanishi, K. Ishikawa, H. Takezoe, M. Yamashita, and K. Kawase, Phys. Rev. E **71**, 061701 (2005).
[13] J. W. Goodby, M. A. Waugh, S. M. Stein, E. Chin, R. Pindak, and J. S. Patel, Nature (London) **337**, 449 (1989).
[14] D. Earl, M. A. Osipov, Y. Takanishi, H. Takezoe, and M. Wilson, Phys. Rev. E **71**, 021706 (2005).
[15] D. A. Coleman, J. Fernsler, N. Chattham, M. Nakata, Y. Takanishi, E. Körblova, D. R. Link, R.-F. Shao, W. G. Jang, J. E. Maclennan, O. Mondainn-Monval, C. Boyer, W. Weissflog, G. Pelzl, L.-C. Chien, J. Zasadzinski, J. Watanabe, D. M. Walba, H. Takezoe, and N. A. Clark, Science **301**, 1204 (2003).
[16] S. W. Choi, M. Zennyoji, Y. Takanishi, H. Takezoe, T. Niori, and J. Watanabe, Mol. Cryst. Liq. Cryst. Sci. Technol., Sect. A **328**, 185 (1999).
[17] J. Watanabe, T. Izumi, T. Niori, M. Zennyoji, Y. Takanishi, and H. Takezoe, Mol. Cryst. Liq. Cryst. Sci. Technol., Sect. A **346**, 77 (2000).
[18] T. Izumi, S. Kang, T. Niori, Y. Takanishi, H. Takezoe, and J. Watanabe, Jpn. J. Appl. Phys., Part 1 **45**, 1506 (2006).
[19] A. Iida, T. Noma, and H. Miyata, Jpn. J. Appl. Phys. **35**, 160 (1996).
[20] Y. Takanishi, T. Izumi, J. Watanabe, K. Ishikawa, H. Takezoe, and A. Iida, J. Mater. Chem. **9**, 2771 (1999).
[21] Y. Takanishi, T. Ogasawara, K. Ishikawa, H. Takezoe, J. Watanabe, Y. Takahashi, and A. Iida, Phys. Rev. E **68**, 011706 (2003).
[22] A. Abe, Macromolecules **17**, 2280 (1984).
[23] J. Watanabe and M. Hayashi, Macromolecules **22**, 4083 (1989).
[24] T. Kusumoto, T. Isozaki, Y. Suzuki, Y. Takanishi, H. Takezoe, A. Fukuda, and T. Hiyama, Jpn. J. Appl. Phys. **34**, L830 (1995).
[25] N. Takada, Master thesis, Tokyo Institute of Technology, 2001 (unpublished).
[26] M. Ozaki, H. Moritake, K. Nakayama, and K. Yoshino, Jpn. J. Appl. Phys. **33**, L1620 (1994).
[27] A. J. Leadbetter and P. G. Wrighton, J. Phys. Colloq. **40**, C3 (1979).
[28] S. Faetti, L. Fronzoni, and P. A. Rolla, J. Chem. Phys. **79**, 5054 (1983).
[29] W. Weissflog, I. Wirth, S. Diele, G. Pelzl, H. Schmalfuss, T. Schoss, and A. Würlinger, Liq. Cryst. **28**, 1603 (2001).
[30] H. N. S. Murthy and B. K. Sadashiva, Liq. Cryst. **29**, 1223 (2002).
[31] J. C. Rouillon, J. P. Marcerou, M. Laguerre, H. T. Nguyen, and M. F. Achard, J. Mater. Chem. **11**, 2946 (2001).
[32] S. Diele, G. Pelzl, and W. Weissflog, Liq. Cryst. Today **9**, 8 (1999).
[33] H. N. S. Murthy and B. K. Sadashiva, J. Mater. Chem. **14**, 2813 (2004).
[34] In the B1 phase, both cases that molecules are tilted and nontilted are observed recently, as in K. Pelz, W. Weissflog, U. Baumeister, and S. Diele, Liq. Cryst. **30**, 1151 (2003).
[35] E. Gorecka, N. Vaupotic, D. Pociecha, M. Cepic, and J. Mieczkowski, ChemPhysChem **6**, 1087 (2005).
[36] R. A. Reddy, V. A. Raghunathan, and B. K. Sadashiva, Chem. Mater. **17**, 274 (2005).